Available online at www.sciencedirect.com
SCIENCE DIRECT
Earth and Planetary Science Letters 245 (2006) 365–372
EPSL
www.elsevier.com/locate/epsl

Deformation in the Jura Mountains (France): First results from semi-permanent GPS measurements

Andrea Walpersdorf [a,*], Stéphane Baize [b], Eric Calais [c], Paul Tregoning [d], Jean-Mathieu Nocquet [e]

[a] *Laboratoire de Géophysique Interne et Tectonophysique, Joseph Fourier University, Maison des Géosciences, BP 53, 38041 Grenoble Cedex 9, France*
[b] *IRSN-Seismic Hazard Division, France*
[c] *Purdue University, West Lafayette, IND, USA*
[d] *Research School of Earth Sciences, The Australian National University, Canberra, Australia*
[e] *Géosciences Azur, Valbonne, France*

Received 13 May 2005; received in revised form 24 January 2006; accepted 20 February 2006
Available online 11 April 2006
Editor: V. Courtillot

Abstract

New GPS estimates of relative motion across the Jura Mountain Belt with respect to the Eurasian Plate indicate less than 1 mm/yr of convergence, considerably less than previous estimates. Velocity uncertainties have been evaluated by several methods and range from 0.2 to 0.5 mm/yr for the semi-permanent stations. The major, statistically-significant strain feature inferred by the Jura GPS measurements is along-arc extension, compatible with tectonic studies. That the detected deformation is small in magnitude highlights two important issues: previous estimates are over-stated and that the approach of using semi-permanent GPS installations is capable of detecting small tectonic signals. Using the upper bound as the rate of convergence, we estimate that this would generate an earthquake of magnitude 5–5.5 every 15 to 75 yr.

Keywords: GPS; Jura; Alps; slow deformation; seismic hazard; semi-permanent GPS installations

1. Introduction

Although France has low to moderate seismotectonic activity, several earthquakes of Ml>5 are recorded in historical catalogues [1] and by paleoearthquake evidence (e.g. [2]). Most of France behaves as a rigid block with internal deformation of no more than 0.5 mm/yr [3].

The Alpine region is the most deforming part of France, where the kinematics are characterized by a radial extension in the internal Alps and perpendicular compression in the forelands [4]. The velocity field and pattern of deformation are clearly influenced by the vicinity of the Eurasian–African plate boundary but the controlling processes of the strain pattern are still a matter of debate.

The Jura area, located between the alpine orogen and its foreland, is known to have been an active area during the Neogene. Some evidence suggests that this is still the case, but precise knowledge of deformation and slip rates is still unavailable. A local GPS network was installed to

* Corresponding author. Tel.: +33 4 76 82 81 04; fax: +33 4 76 82 81 01.
E-mail addresses: andrea.walpersdorf@obs.ujf-grenoble.fr (A. Walpersdorf), stephane.baize@irsn.fr (S. Baize).

0012-821X/$ - see front matter © 2006 Elsevier B.V. All rights reserved.
doi:10.1016/j.epsl.2006.02.037

address this issue and to improve the seismic hazard assessment of the region. Here we present deformation estimates from four years of GPS data observed on six semi-permanent sites.

2. Structural and active tectonics settings

The Jura is the youngest external fold-and-thrust belt related to Alpine orogeny, where faulting and folding began during Miocene [5]. The thrusting of the frontal Jura over its foreland (Bresse graben) occurred during Mio–Pliocene and a total shortening of 30 km occurred over the whole Jura [6]. The most prominent feature of the Jura tectonics is the thin-skin style, with faults and folds rooted into a decollement level (Triassic salt layers). The implication of the basement in the deformation is still debated (e.g. [7]). Most of the models refer to various indenters to explain the fan-shape of the stress/strain orientation pattern and the overall shape and the curvature of the belt.

The current stress/strain pattern is similar to that during the Mio–Pliocene [8]. Shortening and mountain building in the Jura still appear active, mainly within the internal zones [7]. Some neotectonic evidence is reported in the Jura [9], such as in La Balme de Sillingy along the Vuache fault. This fault is currently seismically active with focal mechanisms that reveal left-lateral displacements along NW–SE planes (Fig. 1). The last event occurred on July 15, 1996 at Epagny, close to Annecy (Ml = 5.3), at a depth of 2 km [10]. The French historical catalogue includes several destructive earthquakes that also occurred along the Vuache fault (11/08/1839 in Annecy; 17/04/1936 in Frangy, both with similar surface effects and damage). Elsewhere in the southern Jura the seismicity appears more diffuse except on other NW–SE faults, the Culoz fault for example (Fig. 1).

Slip rates on Jura faults are poorly documented. Estimates of the cumulative lateral offset on the Vuache Fault vary from 1 [10] to 12 km [11], inferring a mean slip rate ranging from 0.5 to 4.4 mm/yr, respectively.

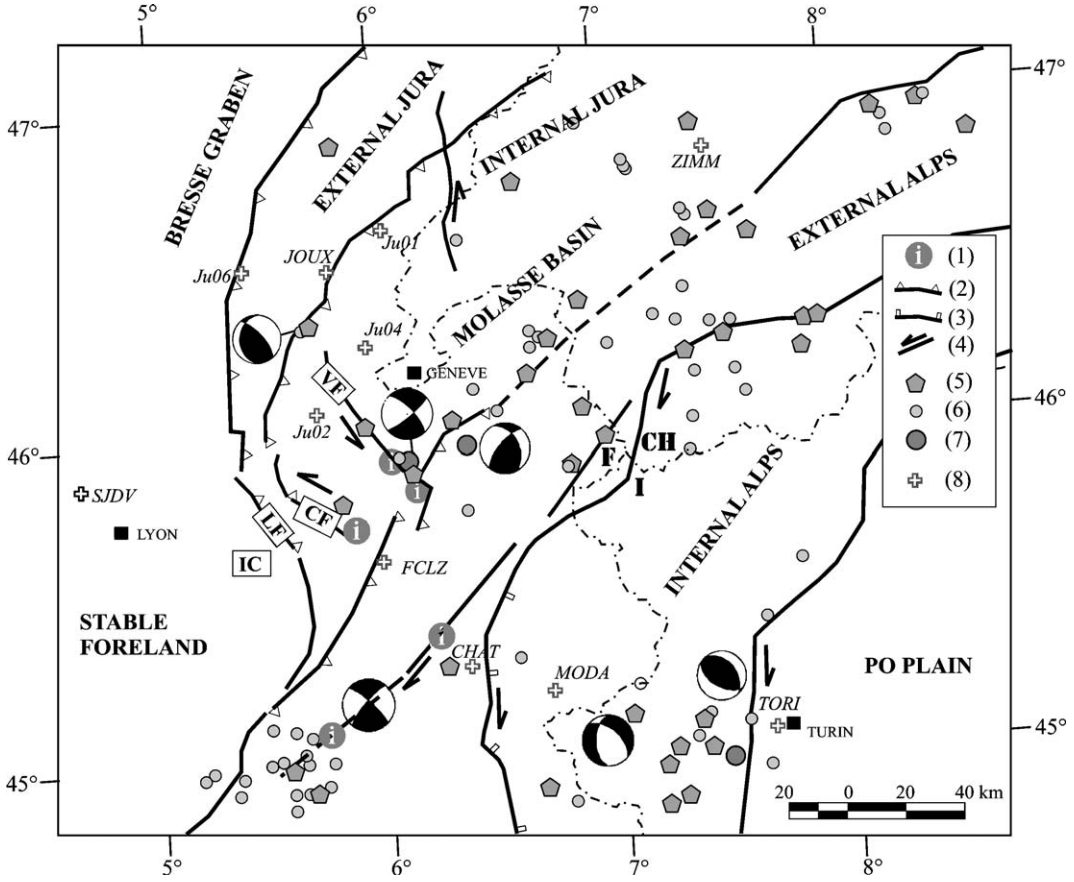

Fig. 1. Active deformation of the Jura Mountains. (1) Reliable neotectonic evidences (see Baize et al., [9] for a synthesis); (2) reverse, (3) normal, (4) strike-slip faulting. (5) Historical epicenters of earthquakes (www.sisfrance.fr). Current seismicity from CEA/LDG (unpublished): (6) 4 < Ml < 5; (7) Ml > 5. VF: Vuache Fault; CF: Culoz Fault; LF: Lagnieu Fault; IC: Ile Crémieu.

Previous geodetic studies using triangulation and GPS data estimated high relative velocities (several mm/yr) within the External Alps and the Jura relative to stable Europe (e.g. [12]), including a drastic shortening in the southern Jura (3–4 mm/yr).

3. GPS processing and results

The 6 semi-permanent sites were each observed over a 10 day period, once or twice per year from May 2000 to August 2004. The sites were selected in order to span 6 tectonic blocks separated by the faults thought to be active (Figs. 1 and 2). The data of these sites are added to those of 18 (in 2000) to 25 (in 2004) sites in the REGAL network (http://kreiz.unice.fr/regal) combined with data from 31 continuously operating sites in western Europe. Site coordinates, orbital parameters, Earth Orientation Parameters, zenith tropospheric delays (13 per day) were estimated using the GAMIT software [13] to generate daily fiducial-free estimates of a polyhedron of sites. These solutions were subsequently combined using GLOBK [14] to estimate a time-evolving polyhedron and time-series of daily site coordinates. Further details of the GPS analysis are given in the Appendix.

We included additional observations on some permanent sites in the REGAL network, commencing in 1997. The additional data prior to the commencement of the Jura network was required in order to obtain stable velocity estimates of the REGAL sites that were consistent with those of Nocquet and Calais [15], derived from REGAL data up to the end of 2001. The Jura velocities

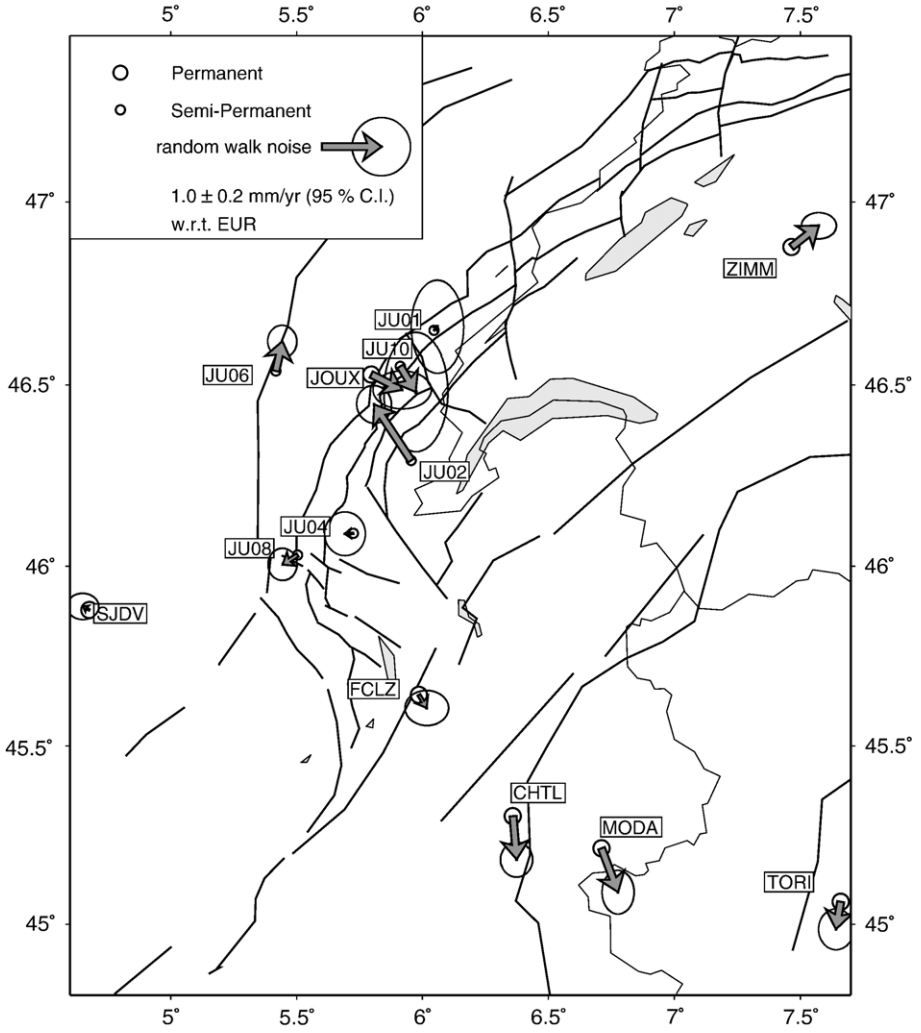

Fig. 2. Velocities of the Jura semi-permanent GPS network relative to the Eurasian Plate. Black lines indicate the faults delimiting the individual tectonical blocks in the region.

(Table 1) were then transformed into a reference frame with respect to stable Eurasia (see Appendix).

Different strategies have been applied to establish realistic estimates of the velocity uncertainties of the semi-permanent stations (see Appendix). These tests suggest that the Jura site velocities have a precision of 0.2–0.5 mm/yr (95% confidence level). The individual velocities in the semi-permanent network show relative motion of 0.1–1.1 mm/yr with respect to stable Eurasia (Table 1) and are barely statistically significant at the 95% confidence level.

4. Discussion

The "tectonic signal" of deformation between the Jura Mountains and the Eurasian reference frame is barely detectable over the noise of the GPS analysis. In addition, there may still be a need for further observations on JU08 and JU10 before the velocity estimates stabilize (see Appendix, Fig. A.3). The uncertainties calculated by applying a site-by-site random-walk noise model are probably realistic and only a few points show relative motion significantly different from zero at the 95% confidence level. Thus, the main result of our analysis is that most of the Jura displacement rates are lower than the present level of uncertainty (0.2–0.5 mm/yr) and that the estimates of 3–4 mm/yr of overall shortening for the Jura Mountains [16,17,12] are too high. This supports the findings of Nocquet and Calais [15].

Strain calculated over the 6 semi-permanent stations and the permanent station JOUX is presented in Table 2 for the solutions with and without random-walk noise. Both solutions show arc-parallel extension but only the solution without random-walk noise shows significant NW–SE compression, compatible with stress measurements [8]. When adding random-walk noise, the major strain feature is the extension along-arc, while the arc-perpendicular compressive component becomes insignificant.

Table 1
Jura site velocities with respect to the Eurasian Plate and in ITRF2000

Eurasia			ITRF2000		Sigma	
(mm/yr)			(mm/yr)		(mm/yr)	
Site	Vel N	Vel E	Vel N	Vel E	Vel N	Vel E
CHTL	−0.73	0.06	14.03	20.45	±0.12	±0.11
FCLZ	−0.22	0.13	14.52	20.37	±0.12	±0.15
JOUX	−0.26	0.52	14.51	20.52	±0.13	±0.20
JU01	0.06	0.06	14.88	20.08	±0.32	±0.18
JU02	0.94	−0.62	15.70	19.50	±0.13	±0.12
JU04	−0.01	−0.14	14.81	19.96	±0.15	±0.14
JU06	0.50	0.11	15.27	19.99	±0.11	±0.11
JU08	−0.16	−0.25	14.68	19.79	±0.11	±0.10
JU10	−0.43	0.26	14.42	20.23	±0.41	±0.22
MODA	−0.74	0.28	14.04	20.79	±0.15	±0.11
SJDV	0.06	−0.11	14.87	19.88	±0.09	±0.11
TORI	−0.46	−0.08	14.22	20.61	±0.14	±0.12

Table 2
Jura strain tensors, with and without random walk noise

Solution	Eps1 [1E-8]	Eps2 [1E-8]	Az (°)
Stochastic	5.6±2.4	−0.2±3.2	111±19
Deterministic	4.3±2.9	−6.2±3.2	148±11

Extension is positive, compression negative and the azimuth given is for the most compressive component.

In the most active part of the Jura (the southern end between the Vuache and Lagnieu faults), the differential displacement of JU02 with respect to JU04 (1 mm/yr to NNW) is consistent with left lateral movement along the NW–SE trending faults (Vuache and Droisy faults).

Assuming that the upper bound GPS estimates of relative motion (1 mm/yr) are correct, and assuming a characteristic total width and length of the active fault of 3 and 30 km, one can calculate, using the Wesnousky [18] model, that the mean recurrence time of a magnitude 5–5.5 characteristic earthquake is 15–75 yr. The historical catalogues show earthquakes with the lower limit magnitude (5), but with a recurrence time clearly longer than 15 yr (~50 yr), indicating either that the true relative motion is significantly lower than 1 mm/yr, or that characteristic earthquakes have magnitudes larger than 5–5.5. An alternative explanation would be that part of the total slip is released aseismically.

5. Conclusion

Relative velocities in the Jura Mountains with respect to the Eurasian Plate are <1 mm/yr, with uncertainties in the range of 0.2–0.5 mm/yr. However, the individual site velocities (with respect to Eurasia) need to be interpreted carefully because the results are barely – if at all – significantly different from zero. Nevertheless, with an upper bound of 1 mm/yr, the present-day convergence in the Jura is considerably less than previously thought. If significant, the major strain feature inferred by the Jura GPS measurements is along-arc extension, compatible with previous tectonic studies but with a significantly reduced rate of convergence.

The Jura semi-permanent GPS network requires additional sites to provide sufficient spatial coverage, with a current absence of sites located in the southern end of the Jura belt, between the Culoz fault and the Ile

Crémieu and also where the indenter is thought to push into the pre-Alps nappes or the sub-alpine molasses where deep-seated thrusts are known. While the estimated rates of convergence are near-zero, we show here that semi-permanent networks are capable of producing such results and therefore present a viable alternative to permanent installations for tectonic studies.

Acknowledgements

We are grateful to the colleagues helping to get the Jura semi-permanent network set up and started: F. Jouanne (LGCA Chambéry), F. Mathieu (CEA) and O. Scotti (IRSN). Many thanks to J.L. Combe (Jura Energie Solaire) who is running the measurements. Thanks to two anonymous reviewers for their comments and encouragements.

Appendix A. Estimation of velocity uncertainties for the semi-permanent GPS network

We have paid particular attention to the precise evaluation of the sub-millimetric velocity estimates in the low deformation area of the Jura. In particular, the velocity uncertainties have been evaluated carefully by a realistic calculation strategy and corroborated by a number of different tests which are presented in this Appendix.

We generated coordinate time series for the permanent and semi-permanent stations from the daily solutions spanning 1997 to 2004 and estimate linear velocities. The maximal differences between these displacement rates for the Jura stations are 1.3 and 1.0 mm/yr in the north and east components, respectively. These values give an upper limit of the differential site motions in the Jura region.

Next, we estimated site velocities for all 62 stations (6 semi-permanent sites, 25 REGAL and 31 other European reference sites) applying coloured noise (in the form of random-walk variation of the site coordinates) to account for the non-Gaussian nature of the noise characteristics of GPS data (e.g. [19,20]). The amount of noise was calculated for each individual station from the noise characteristics of the time series with varying integration times. This strategy helps evaluate realistic velocity uncertainties for the GPS stations according to their different observation spans and measurement environments. The average values applied to the 62 stations are 0.5, 0.3 and 2.8 mm^2/yr for the north, east and vertical components, respectively.

We aligned our network with the ITRF2000 by computing 7-parameter transformations of the coordinates and velocities of 18 well known IGS sites (Fig. A.1) to their ITRF2000 values [21]. The velocities of 23 sites were subsequently inverted to solve for the Euler vector representing motion of the Eurasian Plate with respect to ITRF2000. The residual velocities of these 23 sites are less than 1 mm/yr and are shown in Figs. A.1 and A.2. The estimated Euler vector is comparable to previous

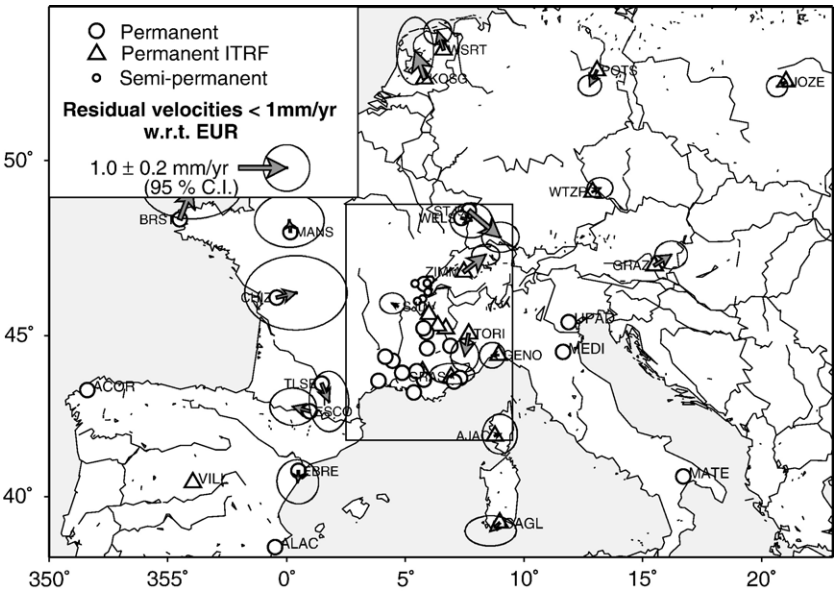

Fig. A.1. GPS stations used in the analysis covering western Europe. Sites used to define the ITRF2000 reference frame are shown by triangles. Velocity vectors are indicated only for stations with residuals of less than 1 mm/yr with respect to the Eurasian Plate, subsequently used to define the Eurasian reference frame. The frame indicates the zoom presented in Fig. A.2.

estimates (Table A.1) and the χ^2 of the inversion for the Euler vector is 1.5.

Following Beavan et al. [23], we computed several velocity solutions with different amounts of random-walk noise applied uniformly to all site coordinates until the χ^2 of the inversion for the Euler vector was close to 1.0. The amount of random-walk noise to be applied to all of the stations to obtain a χ^2 of 1 is 0.5 mm^2/yr for the horizontal coordinates and 3.65×10^3 mm^2/yr on the vertical coordinates (the heights are downweighted in the 7-parameter transformation by a factor 10). The solution without stochastic noise gives a slightly different Euler vector for the Eurasian Plate (Table A.1) from the stochastic solution.

The resulting velocity field with respect to the Eurasian Plate is shown in Fig. A.2 (western Alps), Fig. 2 (zoom on the Jura and environment) and Table 1. The addition of random-walk noise increased the formal uncertainties of the velocity estimates by a factor of 5–10 for continuously recording sites (e.g. SJDV, TORI) but increased the

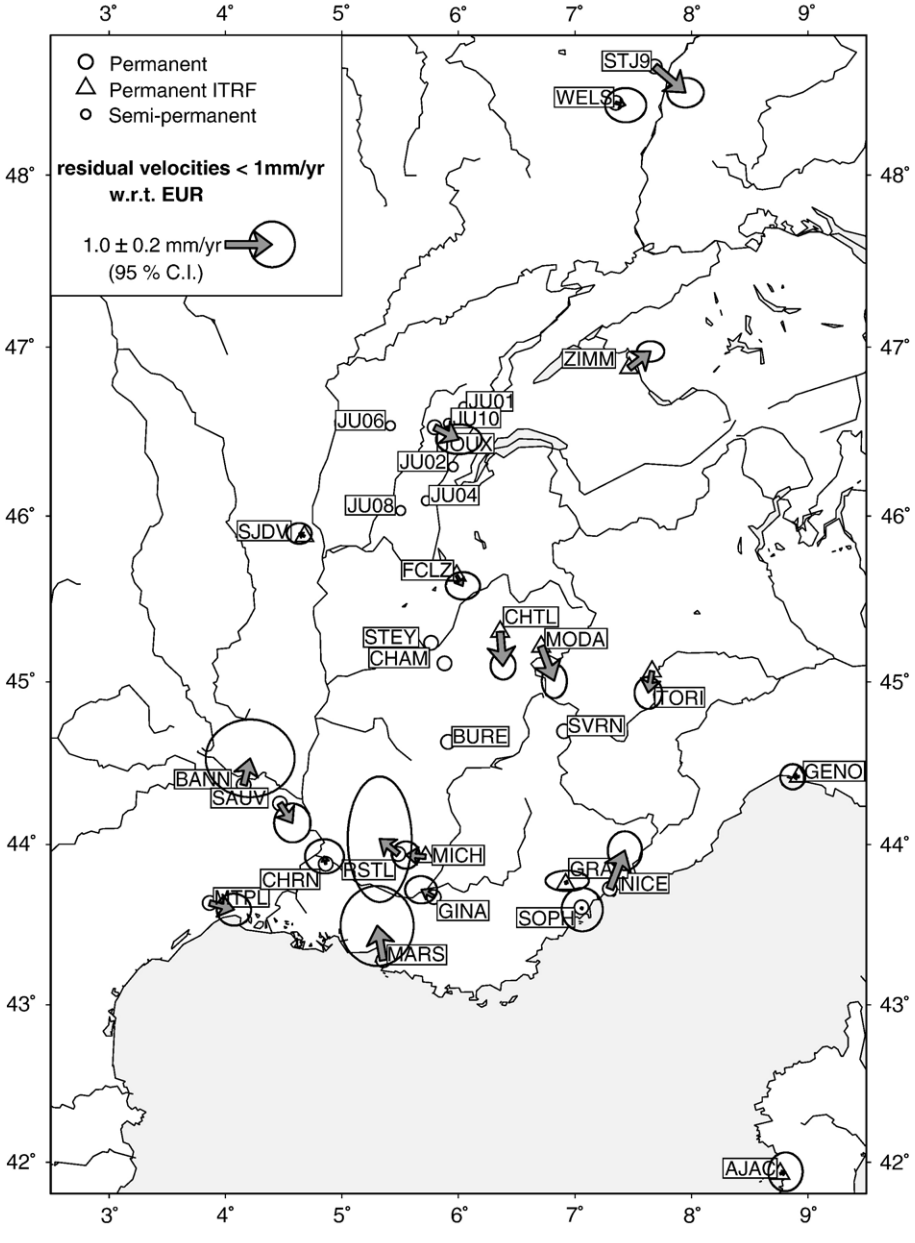

Fig. A.2. Zoom on the western Alps, symbols as in Fig. A.1.

uncertainties of the sites in the Jura region by a factor of 1–3 with respect to the deterministic solution. These increased uncertainties represent a more realistic estimate of the true uncertainties. An average value for the velocity uncertainty of both the semi-permanent and the permanent stations with a span of more than 3 yr is 0.2 mm/yr. The velocity estimates with and without stochastic noise show average differences of 0.2 mm/yr.

What is the effect on the velocity estimates of having campaign-style observations rather than continuous observations? We can explore this by comparing velocity estimates at permanent stations derived using all the data with estimates using only data at the times that Jura sites were observed. Our tests show that the "semi-permanent" velocities for 4 permanent stations differ from the "complete" velocity by less than 0.3 mm/yr (0.24, 0.16, 0.14 and 0.01 mm/yr for FCLZ, GINA, MODA and CHRN respectively). This variation is consistent with our velocity uncertainty estimates derived using coloured noise and can be considered as another estimation of the upper error limit for the true semi-permanent stations. These tests on the formal velocity errors suggest that the uncertainties on horizontal velocities of our semi-permanent stations are between 0.2 and 0.3 mm/yr (95% confidence) after 4 years and up to 8–10 measurement epochs.

Finally, we have checked the stability of the sites velocity estimates as a function of length of observation span. Fig. A.3 shows the evolution of the horizontal velocities of two semi-permanent sites (JU08 and

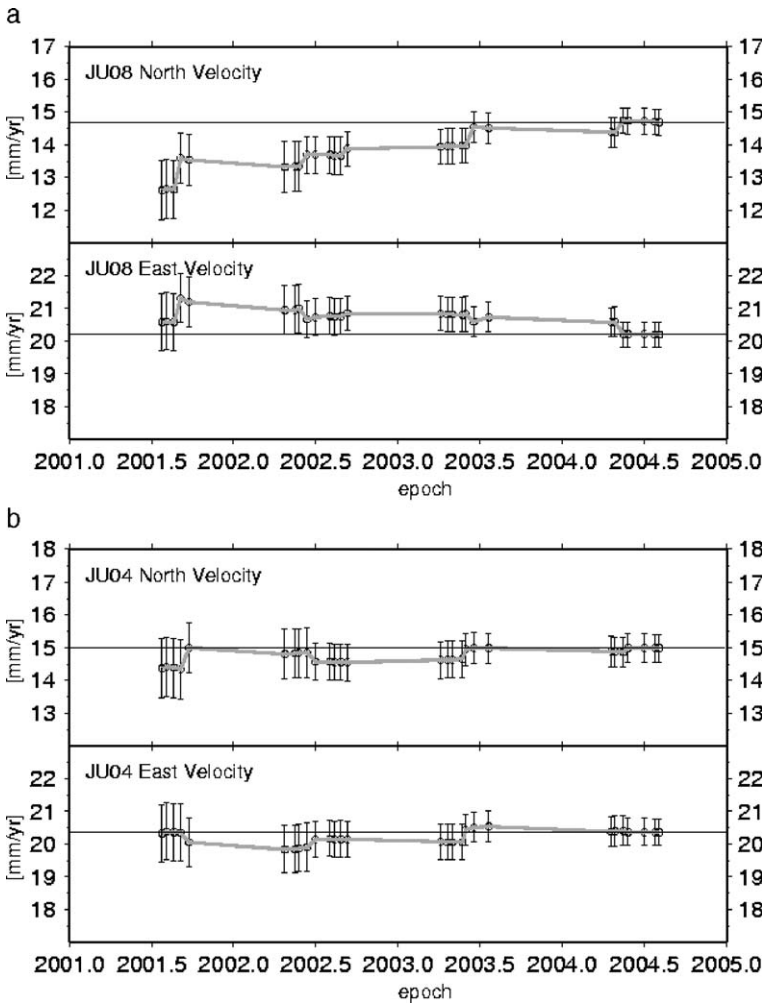

Fig. A.3. Convergence test results for two semi-permanent sites of the Jura network (JU08 and JU04). The dots represent successive estimates of the site velocities, starting from mid-2001 when all sites have been measured at least 3 times. Each new point corresponds to a new measurement epoch of one of the Jura stations. The horizontal line indicates the velocity estimated over the total observation span to the end of 2004. The reference frame is ITRF2000.

JU08) in an ITRF2000 reference frame as more observations are included. The first velocity estimate is shown after three epochs of measurement (epoch 2001.564), each epoch consisting of about 10 24-h GPS measurements. Then, after each new Jura measurement epoch, a new solution was calculated for the whole network. The horizontal line represents the final value in August 2004. The permanent stations SJDV, FCLZ and JOUX, as well as some of the semi-permanent stations (JU02, JU04, JU06) show stable values after epoch 2001.564 at a level of 0.5 mm/yr. JU01 seems to have converged since 2003. However, the semi-permanent sites JU08 and JU10 still have significant rate changes up to the 2004 measurements (in particular for the North component) and their velocity solutions seem to have converged only to a level of 0.5 mm/yr after 4 years of measurement. Clearly, the velocity estimates of some Jura stations (JU01, JU02, JU04, JU06) are more reliable (uncertainties of about 0.2 mm/yr) than others (JU08, JU10, with uncertainties closer to 0.5 mm/yr).

Table A.1
Parameters of the Eurasian Euler pole with respect to ITRF2000

Solution	Lat N (°)	Lon E (°)	Rot. rate (°/My±σ)	Semi-major axis	Semi-minor axis	Azimuth
Stochastic	59.723	−95.492	0.269 ±0.0020	1.09	0.06	69.7
Deterministic	58.040	−99.724	0.262 ±0.0004	0.21	0.02	65.7
Altamimi et al., [21]	57.965	−99.374	0.260			
Sella et al., [22]	58.27	−102.21	0.257			
Nocquet and Calais, [15]	56.0	−101.5	0.25			

References

[1] C. Beauval, O. Scotti, Mapping *b*-values in France using two different magnitude ranges: possible non-power-law model? Geophys. Res. Lett. 30 (17) (2003) 1892, doi: 10.1029/2003GL017576.

[2] M. Sébrier, A. Ghafiri, J.L. Blès, Paleoseismicity in France: fault trench studies in a region of moderate seismicity, J. Geodyn. 24 (1997) 207–217.

[3] J.M. Nocquet, E. Calais, Geodetic measurements of crustal deformation in the western Mediterranean and Europe, Pure Appl. Geophys. 161 (2004), doi: 10.1007/s00024-003-2468-z.

[4] C. Sue, F. Thouvenot, J. Frechet, P. Tricart, Widespread extension in the core of the western Alps revealed by earthquake analysis, J. Geophys. Res. 104 (B11) (1999) 25611–25622.

[5] H.P. Laubscher, Jura kinematics and the Molasse Basin, Eclogae Geol. Helv. 85 (1992) 287–303.

[6] J.L. Mugnier, S. Guellec, G. Ménard, F. Roure, M. Tardy, P. Vialon, Crustal balanced cross-sections through the external Alps deduced from the ECORS profile, in: F. Roure, P. Heitzmann, R. Polino (Eds.), Deep structure of the Alps, Mém. Soc. Géol. France, N. S. n°, vol. 156, 1990, pp. 203–216.

[7] A. Sommaruga, Décollement tectonics in the Jura foreland fold-and-thrust belt, Mar. Pet. Geol. 16 (1999) 111–134.

[8] A. Becker, The Jura Mountains — an active foreland fold-and-thrust belt? Tectonophysics 321 (2000) 381–406.

[9] S. Baize, M. Cushing, F. Lemeille, T. Granier, B. Grellet, D. Carbon, P. Combes, C. Hibsch, Inventaire des indices de rupture affectant le Quarternaire, en relation avec les grandes structures connues, en France métropolitaine et dans les régions limitrophes, Mém. Soc. Géol. Fr. 175 (2002) 142.

[10] F. Thouvenot, J. Fréchet, P. Tapponnier, J.-C. Thomas, B. Le Brun, G. Ménard, R. Lacassin, L. Jenatton, J.R. Grasso, O. Coutant, A. Paul, D. Hatzfeld, The ML 5.3 Épagny (French Alps) earthquake of 1996 July 15: a long-awaited event on the Vuache Fault, Geophys. J. Int. 135 (1998) 876–892.

[11] D. Aubert, Le Risoux, un charriage jurassien de grandes dimensions, Eclogae Geol. Helv. 64 (1971) 151–156.

[12] F. Jouanne, N. Genaudeau, G. Ménard, X. Darmendrail, Estimating present-day displacement fields and tectonic deformation in active mountain belts: an example from the Chartreuse Massif and the southern Jura Mountains, western Alps, Tectonophysics 296 (1998) 403–419.

[13] R.W. King, Y. Bock, Documentation for the GAMIT analysis software, release 10.1, Massachusetts Institute of Technology, Cambridge, MA, 2002.

[14] T.A. Herring, J.L. Davis, I.I. Shapiro, Geodesy by radio interferometry: The application of Kalman filtering to the analysis of very long baseline interferometry data, J. Geophys. Res. 95 (B8) (1990) 12,561–12,581.

[15] J.M. Nocquet, E. Calais, Crustal velocity field of the western Europe from permanent GPS array solutions, 1996–2001, Geophys. J. Int. 154 (2003) 72–88.

[16] J. Martinod, F. Jouanne, J. Taverna, G. Ménard, J.F. Gamond, X. Darmendrail, J.C. Notter, C. Basile, Present-day deformation of the Dauphiné alpine and subalpine massifs (SE France), Geophys. J. Int. 127 (1996) 189–200.

[17] F. Jouanne, G. Menard, D. Jault, Present-day deformation measurements in the French north-western Alps/southern Jura Mountains: data from triangulation comparison, Geophys. J. Int. 119 (1994) 151–169.

[18] S.G. Wesnousky, Earthquakes, quaternary faults, and seismic hazard in California, J. Geophys. Res. 91 (1986) 12587–12631.

[19] A. Mao, C.G.A. Harrison, T.H. Dixon, Noise in GPS coordinate time series, J. Geophys. Res. 104 (1999) 2797–2816.

[20] S.D.P. Williams, Offsets in global positioning system time series, J. Geophys. Res. 108 (B6) (2003) 2310, doi: 10.1029/2002JB002156.

[21] Z. Altamimi, P. Sillard, C. Boucher, ITRF2000: a new release of the International Terrestrial Reference Frame for earth science applications, J. Geophys. Res. 107 (B10) (2002) 2214.

[22] G.F. Sella, T.H. Dixon, A. Mao, REVEL: a model for recent plate velocities from space geodesy, J. Geophys. Res. 107 (B4) (2002) ETG 11-1–ETG 11-32.

[23] J. Beavan, P. Tregoning, M. Bevis, T. Kato, C. Meertens, Motion and rigidity of the Pacific Plate and implications for plate boundary deformation, J. Geophys. Res. 107 (B10) (2002) 2261, doi: 10.1029/2001JB000282.